General Disclaimer

One or more of the Following Statements may affect this Document

- This document has been reproduced from the best copy furnished by the organizational source. It is being released in the interest of making available as much information as possible.

- This document may contain data, which exceeds the sheet parameters. It was furnished in this condition by the organizational source and is the best copy available.

- This document may contain tone-on-tone or color graphs, charts and/or pictures, which have been reproduced in black and white.

- This document is paginated as submitted by the original source.

- Portions of this document are not fully legible due to the historical nature of some of the material. However, it is the best reproduction available from the original submission.

NASA TECHNICAL MEMORANDUM

NASA TM X-73428

NASA TM X-73428

WING SHIELDING OF HIGH-VELOCITY JET AND SHOCK-ASSOCIATED NOISE WITH COLD AND HOT FLOW JETS

by U. von Glahn, D. Groesbeck, and J. Wagner
Lewis Research Center
Cleveland, Ohio 44135

TECHNICAL PAPER to be presented at
Third Aero-Acoustics Conference sponsored by the
American Institute of Aeronautics and Astronautics
Palo Alto, California, July 20-23, 1976

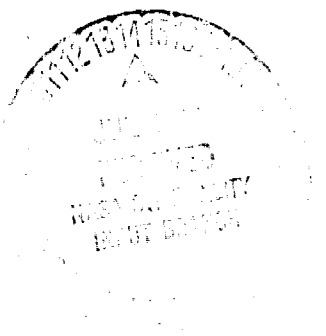

NASA TECHNICAL MEMORANDUM

NASA TM X-73428

NASA TM X-73428

WING SHIELDING OF HIGH-VELOCITY JET AND SHOCK-ASSOCIATED NOISE WITH COLD AND HOT FLOW JETS

by U. von Glahn, D. Groesbeck, and J. Wagner
Lewis Research Center
Cleveland, Ohio 44135

TECHNICAL PAPER to be presented at
Third Aero-Acoustics Conference sponsored by the
American Institute of Aeronautics and Astronautics
Palo Alto, California, July 20-23, 1976

WING SHIELDING OF HIGH-VELOCITY JET AND SHOCK-ASSOCIATED NOISE WITH COLD AND HOT FLOW JETS

U. von Glahn,* D. Groesbeck,** and J. Wagner†
National Aeronautics and Space Administration
Lewis Research Center
Cleveland, Ohio 44135

Abstract

Jet exhaust noise shielding data are presented for cold and hot flows (ambient to 1100 K) and pressure ratios from 1.7 to 2.75. A nominal 9.5-cm diameter conical nozzle was used with simple shielding surfaces that were varied in length from 28.8 to 114.3 cm. The nozzle was located 8.8 cm above the surfaces. The acoustic data with the various shielding lengths are compared to each other and to that for the nozzle alone. In general, short shielding surfaces that provided shielding for subsonic jets did not provide as much shielding for jets with shock noise; however, long shielding surfaces did shield shock noise effectively.

Introduction

The installation of engines over the wing is being considered as part of the overall effort to reduce the level of noise radiated to the ground from high velocity jets such as might be used with supersonic aircraft (fig. 1). By proper orientation of the jet exhaust location considerable shielding of jet noise can be achieved.[1] The principle involved is analogous to the erection, on the ground, of a barrier between a noise source and an observer. For aircraft application, the wing constitutes the barrier and the jet exhaust is considered to be the noise source. The main difference between the two applications of barrier shielding is that the jet exhaust is a distributed noise source along the jet axis, whereas the noise in ground applications is generally considered to be a point noise source. As a consequence, the local noise sources in a jet exhaust that occur at increasingly larger distances downstream from the nozzle are not shielded as well as those near the nozzle because the shielding length provided by the wing decreases with increasing distance from the nozzle. Furthermore, increasingly lower frequency noise is generated in a jet with distance from the nozzle exhaust plane; this again limits the suppression of jet mixing noise by wing shielding because low frequency noise tends to pass through and around barriers whereas high frequency noise is effectively attenuated by a shielding surface. The attenuation results primarily from a redirection of the noise by reflection from the source-side of the barrier. The shielding concept does not result in a change in the generation of the total sound power. Shock noise generates an additional noise source that must be shielded by the wing. It has been shown that shock-associated noise, even at low pressure ratios near 2.0 can cause 10 dB or more noise increases over a wide range of frequencies.[2] The magnitude of the shock-associated noise is a function of the number of shock bottles; hence, pressure ratio.[3]

In Ref. 2, it is shown that when the wing shielding length is about equal to the core length, jet noise shielding occurs at subsonic but not at low supersonic velocities. This implies that the generation of shock noise is associated with the tip region of the jet core. On the basis of these preliminary data, placement of the nozzle exhaust plane some distance ahead of the wing for a supersonic aircraft (fig. 1(b)) could perhaps be considered and still shield the ground observer from shock-associated noise. Consequently, as part of this program, acoustic data were obtained with the nozzle exhaust plane located about 5 nozzle diameters ahead of the wing leading edge. (Herein, the terms "shielding surface" and "wing" are used interchangeably.)

In the present paper, the results from a study of jet exhaust noise shielding are presented for both cold (ambient) and hot flow jets (up to 1100 K) for pressure ratios from 1.7 to 2.75. A nominal 9.5 cm conical nozzle was used together with wings (flat boards) of different chord sizes. The wing chords varied from 40.6 to 114.3 cm. The nozzle exhaust plane was placed at chordwise positions relative to the wing leading edge of 11.8 cm downstream and 47.6 cm upstream. The nozzle centerline was located about 13.6 cm above the wing surface for all tests. The wing span was 122 cm.

Acoustic results generally are presented in terms of SPL spectra and OASPL directivity plots.

Apparatus and Procedure

Flow System

The test rig flow system, shown schematically in Fig. 2, is horizontal and consists of the following sections, proceeding in the flow direction from the 1030 kN/m^2 maximum, laboratory air supply: (1) main shut-off valve, (2) flow metering orifice section, (3) flow control valve, (4) valve noise muffling section, (5) com-

*Member AIAA; Jet Acoustics Branch.
**Aerospace Research Engineer.
†Operation Engineer.

WING SHIELDING OF HIGH-VELOCITY JET AND SHOCK-ASSOCIATED NOISE WITH COLD AND HOT FLOW JETS

U. von Glahn,* D. Groesbeck,** and J. Wagner†
National Aeronautics and Space Administration
Lewis Research Center
Cleveland, Ohio 44135

Abstract

Jet exhaust noise shielding data are presented for cold and hot flows (ambient to 1100 K) and pressure ratios from 1.7 to 2.75. A nominal 9.5-cm diameter conical nozzle was used with simple shielding surfaces that were varied in length from 28.8 to 114.3 cm. The nozzle was located 8.8 cm above the surfaces. The acoustic data with the various shielding lengths are compared to each other and to that for the nozzle alone. In general, short shielding surfaces that provided shielding for subsonic jets did not provide as much shielding for jets with shock noise; however, long shielding surfaces did shield shock noise effectively.

Introduction

The installation of engines over the wing is being considered as part of the overall effort to reduce the level of noise radiated to the ground from high velocity jets such as might be used with supersonic aircraft (fig. 1). By proper orientation of the jet exhaust location considerable shielding of jet noise can be achieved. [1] The principle involved is analogous to the erection, on the ground, of a barrier between a noise source and an observer. For aircraft application, the wing constitutes the barrier and the jet exhaust is considered to be the noise source. The main difference between the two applications of barrier shielding is that the jet exhaust is a distributed noise source along the jet axis, whereas the noise in ground applications is generally considered to be a point noise source. As a consequence, the local noise sources in a jet exhaust that occur at increasingly larger distances downstream from the nozzle are not shielded as well as those near the nozzle because the shielding length provided by the wing decreases with increasing distance from the nozzle. Furthermore, increasingly lower frequency noise is generated in a jet with distance from the nozzle exhaust plane; this again limits the suppression of jet mixing noise by wing shielding because low frequency noise tends to pass through and around barriers whereas high frequency noise is effectively attenuated by a shielding surface. The attenuation results primarily from a redirection of the noise by reflection from the source-side of the barrier. The shielding concept does not result in a change in the generation of the total sound power. Shock noise generates an additional noise source that must be shielded by the wing. It has been shown that shock-associated noise, even at low pressure ratios near 2.0 can cause 10 dB or more noise increases over a wide range of frequencies. [2] The magnitude of the shock-associated noise is a function of the number of shock bottles; hence, pressure ratio. [3]

In Ref. 2, it is shown that when the wing shielding length is about equal to the core length, jet noise shielding occurs at subsonic but not at low supersonic velocities. This implies that the generation of shock noise is associated with the tip region of the jet core. On the basis of these preliminary data, placement of the nozzle exhaust plane some distance ahead of the wing for a supersonic aircraft (fig. 1(b)) could perhaps be considered and still shield the ground observer from shock-associated noise. Consequently, as part of this program, acoustic data were obtained with the nozzle exhaust plane located about 5 nozzle diameters ahead of the wing leading edge. (Herein, the terms "shielding surface" and "wing" are used interchangeably.)

In the present paper, the results from a study of jet exhaust noise shielding are presented for both cold (ambient) and hot flow jets (up to 1100 K) for pressure ratios from 1.7 to 2.75. A nominal 9.5 cm conical nozzle was used together with wings (flat boards) of different chord sizes. The wing chords varied from 40.6 to 114.3 cm. The nozzle exhaust plane was placed at chordwise positions relative to the wing leading edge of 11.8 cm downstream and 47.6 cm upstream. The nozzle centerline was located about 13.6 cm above the wing surface for all tests. The wing span was 122 cm.

Acoustic results generally are presented in terms of SPL spectra and OASPL directivity plots.

Apparatus and Procedure

Flow System

The test rig flow system, shown schematically in Fig. 2, is horizontal and consists of the following sections, proceeding in the flow direction from the 1030 kN/m^2 maximum, laboratory air supply: (1) main shut-off valve, (2) flow metering orifice section, (3) flow control valve, (4) valve noise muffling section, (5) com-

*Member AIAA; Jet Acoustics Branch.
**Aerospace Research Engineer.
†Operation Engineer.

bustor, (6) combustor noise muffling section, (7) nozzle isolation pipe, and (8) conical nozzle.

The valve noise muffling section consists of a perforated plate immediately downstream of the flow control valve, followed by a labyrinth type absorptive muffler.

The combustor is a modified Pratt & Whitney J-57 engine combustor can installed in a section of 30.3 cm diameter pipe. The combustor is supplied with aviation fuel type A-1.

The combustor noise muffling section consists of a perforated cone immediately downstream of the combustor, followed by an absorptive muffler.

A 30.3 cm i.d. isolation pipe extends downstream 6.18 m from the muffler, terminating at the nozzle. An acoustic and thermal insulation liner is installed in the isolation pipe.

Nozzle

The nozzle consisted of a flanged truncated cone 30.5 cm i.d. at the large end and 9.54 cm i.d. at the discharge end. The overall length of the nozzle is 65.2 cm. The nozzle centerline is horizontal and 1.7 m above ground level.

Nozzle pressure ratio was manually controlled with the flow control throttling valve. Nozzle discharge temperature was established by manual control of fuel flow to the combustor.

For the present program, pressure ratios across the nozzle of 1.7, 2.1, and 2.75 were used. Jet total temperatures from 283 (ambient) to 1096 K were used.

Acoustic Shields

Three acoustic shields were used in this test program. The dimensions and mounting of the shields are shown in Figs. 3 and 4, respectively. All shields were rectangular plates of 0.625 cm thick by 122 cm wide 304 stainless steel. The total axial lengths of the shields were 40.6, 61.0, and 114.3 cm. For all tests, the shields were mounted vertically with the shield face aligned parallel to and offset a nominal 12.6 cm from the nozzle axis (fig. 3).

The shields were mounted on a structural steel frame cantilevered from the nozzle flange. Two mounting configurations were used: the first allowed the leading edge of the shield to be set 11.8 cm upstream of the nozzle exhaust plane, while the second placed the leading edge of the shield 47.6 cm downstream of the nozzle exhaust plane.

Acoustic Instrumentation and Data Analysis

Far field acoustic measurements were made in an outdoor environment, using a horizontal semicircular array of microphones on a 4.57 m radius, centered on the nozzle exhaust plane and in a plane level with the nozzle centerline. The microphone angles were 40°, 60°, 75°, 90°, 105°, 120°, 135°, and 145° measured from the inlet. A mat of 15 cm thick acoustic foam was placed on the ground (asphalt) inside the microphone array to minimize ground reflections.

The omnidirectional condenser type microphones used were 1.27 cm in diameter having a frequency response flat within 1 dB from 20 Hz to 20 kHz. The microphones were calibrated immediately before and after each run with a piston calibrator which generated a 124 dB, 250 Hz tone. The data is processed through a 1/3 octave spectrum analyzer. The output is recorded on paper tape and/or incremental digital tape.

Three samples of noise data were taken at each microphone for each run condition. Background noise levels were also recorded before and after each test run.

Nozzle-Alone Acoustic Results

In order to relate the shielding benefits obtained with an engine over-the-wing installation, the acoustic characteristics of the nozzle alone will be discussed first. Both the subsonic jet and underexpanded supersonic jet acoustics will be described in order to provide baseline data for the shielded jet operation discussed later.

Subsonic. - The spectral characteristics for the subsonic jet are shown in Fig. 5 in terms of SPL-OASPL plots as a function of an effective jet mixing noise Strouhal number. This effective Strouhal number is similar to that suggested in Ref. 4; however, the temperature dependency T_j/T_a herein has an exponent of 0.25 rather than 0.4 as in Ref. 4. Furthermore, the temperature effect is expressed as a function of C_j/C_a rather than T_j/T_a as in Ref. 4. The data shown in Fig. 5 are for a jet Mach number of 0.94 and for directivity angles, θ, of 60°, 90°, and 120°. The solid curve through the data is taken from Ref. 5. In general good agreement is observed except at effective Strouhal numbers less than 0.1 where the experimental data is up to 3 dB higher than the curve from Ref. 5. At a directivity angle of 120°, the hot flow data at the high frequencies (>10 000 Hz) are somewhat lower than the cold flow data. At larger directivity angles of 135° and 145° (not shown) this effect became more pronounced.

Similar trends were obtained at other directivity angles (40°, 75°, and 105°) and lower jet Mach numbers (data not included herein).

The OASPL values, shown in Fig. 6, were correlated in the manner suggested in Ref. 4. The data shown are for a directivity angle of 90^{o}. It is apparent that the data correlate well with the parameters developed in Ref. 4.

Shock noise. - Operation of a nozzle at above choking pressure ratios (1.89) produces an underexpanded supersonic jet. The total noise spectrum is considered to be composed of jet mixing noise and by shock-associated noise. The supersonic jet noise can be calculated by logarithmically accounting for the noise contributed by each source. This procedure, which is used herein, is based on the assumption that jet mixing noise and shock noise are independent of each other.

Typical spectra for shock-associated noise are shown in Fig. 7 for various directivity angles and a jet Mach number of 1.3. The data are for an ambient jet temperature, but the data trends shown are representative also of hot flow. The solid curve in the figure indicates the variation in the location of the peak frequency for the shock noise component. With increasing directivity angle, the peak frequency of the shock noise is seen to increase.

The shock noise spectra for the nozzle only was isolated by subtracting antilogarithmically the SPL due to the jet mixing noise from the SPL of the total spectrum for each test condition. In Figs. 8 to 10 representative shock noise spectra obtained by this procedure are shown plotted as a function of a shock-noise Strouhal number for various jet total temperatures and directivity angles. The shock Strouhal number, ST_s, used is given by the relationship:

$$ST_s = \frac{f_s D}{U_j}\left[\beta\left(1 + 0.62\,\frac{U_j}{C_a}\cos\theta\right)\right] \qquad (1)$$

where

$$\beta = \sqrt{M_j^2 - 1}$$

At a 90^{o} directivity angle, Eq. (1) simplifies to:

$$ST_s = \frac{f_s D}{U_j}(\beta) \qquad (2)$$

The effect of directivity angle on the shock noise spectra is shown in Fig. 8 for jet total temperatures of 283 and 578 K and an M_j of 1.3. The shock noise level, as expected, is omnidirectional.

The effect of jet total temperature on shock noise spectra is shown in Fig. 9 for directivity angles of 60^{o}, 90^{o}, and 120^{o} and an M_j of 1.3. In all cases, the hot flow data have higher SPL values than those for cold flow. The differences in SPL between hot flow and cold flow are from 2 to generally 5 dB.

With a lower supersonic flow ($M_j = 1.09$) only limited shock spectra at $\theta = 60^{o}$ were obtainable because the mixing noise at greater directivity angles and with hot flow almost completely dominated the spectra. The limited shock spectral data at $\theta = 60^{o}$ are shown in Fig. 10 and indicate a reversal of trends discussed for an M_j of 1.3 (fig. 9). With increasing jet total temperature the measured shock noise appears to decrease; however, because of the difficulty in separating the mixing noise from the shock noise with hot flow at $M_j = 1.09$ the data trend shown in Fig. 10 may not be representative.

Although the levels of the shock spectra appear to be temperature dependent, the shock Strouhal number (eq. (1)) does appear to correlate the frequency shift with directivity angle. The shock peak frequency is obtained by setting Eq. (1) equal to 0.85.

The directional variation of the peak frequency for shock noise spectra is illustrated in Fig. 11. The curves shown are based on Eq. (1) with a shock Strouhal number equal to 0.85. With increasing jet Mach number (M_j) the shock peak frequency decreases. Also, with increasing temperature ratio, T_j/T_a, the shock peak frequency increases.

Finally, in Fig. 12 the variation of OASPL with directivity angle is shown for both subsonic and supersonic flow and for jet total temperatures of 283 (cold flow), 751, and 1096 K. As would be expected, with increasing M_j, the OASPL increases. With cold flow, the OASPL for supersonic velocities is nearly constant for all directivity angles shown. Jet mixing noise begins to dominate shock noise only at directivity angles greater than about 110^{o}. With increasing jet total temperature, the jet mixing noise at the low supersonic flow tends to dominate the shock noise and the OASPL variation with directivity angles resembles that for subsonic jet mixing noise. At the highest M_j of 1.3, shock noise dominates only in the forward quadrant ($\theta < 80^{o}$) at the highest jet total temperature (1096 K).

Nozzle Over Wing

In examining the effect of shielding on supersonic jet noise, the subsonic jet acoustic characteristics will be used as a reference or baseline for the discussion of noise level changes and trends with shielding surface geometry. The following sections will first summarize the subsonic jet nozzle/wing acoustic characteristics and then those determined for the supersonic jet nozzle/wing operation. In all cases, the jet nozzle/wing acoustics will be compared with the appropriate nozzle-alone acoustics.

Subsonic

Spectra. - The effect of wing shielding on the nozzle/wing spectra at a jet Mach number of 0.94 is shown in Fig. 13 for a directivity angle of 60°. The spectra shown are for jet total temperatures of 283 (cold flow), 751, and 1096 K. With increasing surface (wing) length, the jet/surface interaction noise in the low and mid frequency range (<2500 Hz) increases (see also ref. 5).

The ΔSPL at the peak (SPL-SPL_N) in the low frequency range occurs at about 300 Hz and is independent of jet temperature. The peak SPL increases with U_j^3. In the mid frequency range (500 to 2500 Hz) the jet/surface interaction noise increases with increasing temperature (jet velocity). The jet noise attenuation due to the presence of the shielding surface increases with increasing surface length in the high frequency range (1250 to 2000 Hz), as would be expected.

The subsonic jet data trends shown in Fig. 13 for the 60° directivity angle also apply generally to the remaining directivity angles (40° to 145°) included in this study. The hot and cold flow subsonic data from the present study also generally confirm the data trends of the cold flow, smaller model scale (one-half) test data reported in detail in Ref. 2.

OASPL. - Representative data showing the variation of OASPL for nozzle/wing configurations as a function of directivity angle are shown in Fig. 14 for jet total temperatures of 283 and 1096 K. The data shown are for an M_j of 0.94. With cold flow (283 K) the interaction noise in the low and mid frequency ranges is sufficiently high compared with jet mixing noise attenuation at high frequencies by wing shielding that only at θ values of 135° and 145° are the OASPL values with the longest shielding surface (102.5 cm) below those for the nozzle only (<1 dB). The OASPL values with the shorter shielding lengths of 28.8 and 49.2 cm generally are somewhat greater than those for the nozzle only because the effect of the interaction noise greatly exceed the shielding benefits. With increasing temperature, significantly larger OASPL reductions, compared with nozzle only values were obtained. The OASPL values shown in Fig. 14 for a jet total temperature of 1096 K indicate OASPL reductions with the longest shielding surface (102.5 cm), compared with nozzle only values, beginning at a directivity angle of 75° and reaching ΔdB values of 10 dB at θ equal to 135° and 145°. The shorter shielding surfaces provided much less of a reduction in OASPL (fig. 14). The reductions in OASPL obtained with a T_j of 1096 K are the result of the high frequency jet-mixing SPL values being larger than the low frequency interaction noise; consequently, a reduction of the high frequency noise levels by wing shielding is accompanied by a significant reduction in OASPL.

Supersonic

Spectra. - Representative data illustrating wing shielding of a supersonic jet are shown in Figs. 15 to 18.

In Fig. 15 the effect of wing shielding on the SPL for a supersonic jet operating at an M_j of 1.09 is shown for a directivity angle of 60° and jet total temperatures of 283 and 1096 K. In the low and mid frequency ranges (<2000 Hz) the acoustic levels and trends are governed by jet mixing considerations since shock noise for the present configurations are generally associated with frequencies greater than 2000 Hz (figs. 9 and 10). Consequently, the spectral changes and data trends with supersonic jet velocities at the frequencies are similar to those for subsonic jet velocities. A significant difference is apparent in the amount of high frequency jet noise suppression with shielding lengths of 28.8 and 102.5 cm obtained with supersonic flow compared with that for subsonic flow. With supersonic flow, less jet noise attenuation is obtained than with subsonic flow for these surface lengths. This phenomena is even more apparent in Fig. 16 in which the SPL data for an M_j of 1.3 is shown for the same jet total temperatures as in Fig. 15. The apparent loss in noise suppression is essentially independent of jet total temperature. With the longest shielding surface (102.5 cm), jet noise suppression of similar magnitudes for both subsonic and supersonic flow are obtained at high frequencies (>2000 Hz). At larger directivity angles (fig. 17; θ, 90° and fig. 18; θ, 120°) generally similar acoustic data trends were observed. The inability to suppress the high frequency noise with the smaller shielding surfaces is even more apparent at these directivity angies.

It is evident from the acoustic data presented in Figs. 15 to 18 that with increasing jet Mach number the shock noise, associated with the higher frequencies in the spectra, is not shielded by surfaces that do shield jet mixing noise in the same frequency range at subsonic jet velocities. Because the core length increases with jet Mach number[6] it is likely that the shock noise is generated near or even beyond the trailing edge of the shorter shielding surfaces; consequently, no significant acoustic shielding occurs. With the longest shielding surface (102.5 cm) the shock noise and some jet mixing noise is shielded.

OASPL. - Representative variations of OASPL with directivity angle are shown in Fig. 19 for a jet total temperature of 1096 K and a jet Mach number of 1.3. Data are shown for shielding surface lengths of 28.8, 49.2, and 102.5 cm and the nozzle only. It is apparent that with the shorter shielding lengths, no OASPL reductions, compared with nozzle only data, are obtained.

As in the case for subsonic flow, the low frequency interaction noise effectively cancels out any reductions in high frequency shock noise due to wing shielding. With the longest shielding surface, however, the shock noise is sufficiently attenuated by wing shielding to provide net reductions in OASPL compared with the nozzle only values.

Nozzle Ahead of Wing

Because the short wings (shielding surface lengths of 28.8 and 49.2 cm) did not provide significant shock noise shielding, indicating that shock noise was associated with the core-tip region of the jet, it was speculated that the shielding surface could be moved downstream from the original nozzle location (fig. 3). This could then possibly provide a suitable shielding surface with the short wings for the shock noise component of the nozzle/wing spectra. Consequently, the nozzle was moved 5 diameters upstream of the leading edge of the wing. In a real application this would permit cantilevering some or all of the engines from the aircraft fuselage with the nozzle exhaust plane above and ahead of the wing leading edge, thereby permitting greater flexibility in aircraft design and weight distribution (fig. 1(b)).

Spectra. - Representative acoustic spectra obtained from a study of this nozzle-wing placement are shown in Figs. 20 and 21. Data are shown for a jet Mach number of 1.3 and a jet total temperature of 1096 K. Shielding surface (wing) lengths of 40.6 and 114.3 cm were used in obtaining the acoustic data with the nozzle ahead of the wing. Also shown in Figs. 20 and 21, for comparison, are nozzle over the wing data (shielding surface lengths of 28.8 and 102.5, respectively) and nozzle alone curves.

With a short wing (shielding length, 40.6 cm) no jet noise shielding was obtained in the forward quadrant ($\theta = 60^{\circ}$); indeed there was an increase over the entire spectrum compared with that for the nozzle over-the-wing placement and the nozzle only (fig. 20). In the rearward quadrant ($\theta = 120^{\circ}$) essentially no shielding was obtained while the noise level increased at the lower frequencies (<800 Hz). At $\theta = 90^{\circ}$ (not shown) there was a significant increase in noise level at frequencies less than 5000 Hz (up to 13 dB greater than the nozzle-alone SPL values) while for frequencies above 5000 Hz the SPL values were about 1 dB greater than those for the nozzle alone. Similar acoustic results were obtained with subsonic flow of $M_j = 0.94$ (not shown herein).

With a shielding surface length of 114.3 cm and supersonic flow ($M_j = 1.3$) the interaction noise for frequencies less than 500 Hz for the two nozzle placements was about the same (fig. 21). In the mid frequency range, the interaction noise was about equal to that for the nozzle alone SPL values in the forward quadrant ($\theta = 60^{\circ}$ and 90°) and was below that for the nozzle-only values in the rear quadrant ($\theta = 120^{\circ}$). In the rear quadrant the suppressed SPL values were less than those with the nozzle over-the-wing placement. In the high frequency range (>5000 Hz) the SPL values in the forward quadrant were about 2 dB greater than the nozzle-alone values indicating that shock noise shielding was not achieved. In the rear quadrant ($\theta = 120^{\circ}$), shock noise suppression (up to about 8 dB) was obtained at the high frequencies. Lesser amounts of shock noise shielding (2 to 5 dB) were obtained at $\theta = 90^{\circ}$.

Similar acoustic data trends were obtained with jet total temperatures of 283 and 751 K. With lower jet total temperatures the shock noise shielding was somewhat greater (up to 2 to 3 dB) than that shown in Figs. 20 and 21. The improved acoustic shielding at the lower jet total temperatures is attributed to the larger core lengths associated with colder jet flows. Thus, the colder flow shock-noise generation is located axially over the shielding surface which results in improved acoustic shielding characteristics.

OASPL. - A comparison of OASPL for nozzle placements ahead of and over the wing are shown in Fig. 22. The data shown are for a jet total temperature of 1096 K and a jet Mach number of 1.3. Also shown for comparison is the nozzle alone curve. It is apparent, as was the case from the spectral plots, that the OASPL values in the forward quadrant are greater for the nozzle located ahead of the wing than those for either the nozzle alone and the nozzle located over the wing. In the rearward quadrant the nozzle located ahead of the wing yielded significant OASPL reductions compared with the nozzle alone. In fact, at directivity angles of 120° and 135°, the OASPL reductions for the forward nozzle location slightly exceeded those obtained with the nozzle located over the wing.

Concluding Remarks

The results obtained from the present exploratory study showed that short shielding surface lengths (small chord wings) shielded much less high frequency noise generated by shocks than the mixing noise generated by subsonic jets in the same frequency range. With long shielding surfaces (large wings), shock noise was shielded as effectively as jet mixing noise at subsonic jet velocities. The differences between hot and cold flow in terms of noise shielding were not significant and can be accounted for by scaling for velocity on a Strouhal number basis as in Ref. 1.

Placement of the nozzle ahead of the wing provided significant shielding in the rear quadrant; however, no

shielding, and in some cases additional noise, was measured in the forward quadrant. Considering that a supersonic-type commercial aircraft would, in all probability, have a large-chord, delta-type wing and would therefore land and takeoff at large angle settings relative to the ground, placement of engines ahead of and above the wing would realize some shock and jet noise shielding benefits. This, in turn, provides greater flexibility for engine installations and could possibly influence cruise performance compared with engine exhaust nozzle placement over the wing.

The increase in low frequency noise which occurs regardless of wing position must be reduced before jet noise shielding by wing placement can be seriously considered for practical applications for supersonic-type commercial aircraft. The low frequency pressure fluctuations (noise) for a full-scale aircraft cause both a severe local structural fatigue problem and an interior cabin noise problem. The OASPL attenuation at high frequencies by wing shielding would be less significant at full scale since the largest noise reductions occur in the frequency ranges that do not particularly influence the PNL calculations for a real aircraft.

Finally, in the study reported in Ref. 1, it was shown that shock noise is not attenuated significantly in flight. This was demonstrated by free-jet forward speed tests using a conical nozzle with and without wing shielding of jet mixing and shock noise. Any small reductions in shock noise level noted in Ref. 1 are believed due to the source alteration caused by a change in the jet shear layer by airspeed and the consequently modified interaction with the shock waves. When the shock noise was dominated by jet mixing noise, the effect of flight was to reduce the noise level until shock noise became a noise floor. [1]

Nomenclature

(All symbols in SI units unless otherwise noted.)

A_j	nozzle area
C	speed of sound
D	nozzle diameter
f	frequency, Hz
L	total surface length (wing chord)
L_s	shielding surface length
M	Mach number
OASPL	overall sound pressure level, dB re 2×10^{-5} N/m^2
R	distance from noise source to observer
SPL	sound pressure level, dB re 2×10^{-5} N/m^2
ST	Strouhal number
T	temperature
U	flow velocity
β	shock parameter defined by $\sqrt{M_j^2 - 1}$
θ	directivity angle measured from inlet
ρ	density

Subscripts:

a	ambient
ISA	international standard atmosphere, 288 K and 101.3 kN/m^2
j	jet
N	nozzle
p	peak
s	shock

References

1. von Glahn, U., Groesbeck, D., and Reshotko, M., "Geometry Considerations for Jet Noise Shielding With CTOL Engine-Over-the-Wing Concept," TM X-71562, 1974, NASA.

2. von Glahn, U. and Goodykoontz, J., "Installation and Airspeed Effects on Jet Shock-Associated Noise," TM X-71792, 1975, NASA.

3. Harper-Bourne, M. and Fisher, M. J., "The Noise from Shock Waves in Supersonic Jets," Noise Mechanisms, AGARD-CP-131, Advisory Group for Aerospace Research and Development, Paris (France), 1973.

4. Stone, J. R., "Interim Prediction Method for Jet Noise," TM X-71618, 1974, NASA.

5. Olsen, W. and Friedman, R., "Jet Noise From Co-Axial Nozzles Over a Wide Range of Geometric and Flow Parameters," AIAA Paper 74-43, Washington, D.C., 1974.

6. Nagamatsu, H. and Horvay, G., "Supersonic Jet Noise," AIAA Paper 70-237, New York, N.Y., 1970.

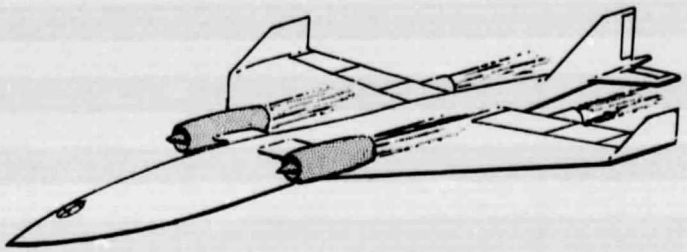

(a) JET EXHAUST NOZZLE PLACEMENT OVER THE WING.

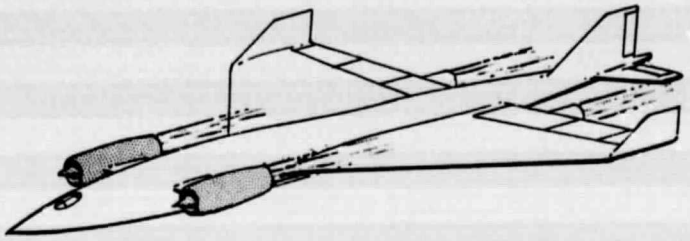

(b) JET EXHAUST NOZZLE PLACEMENT AHEAD OF WING.

Figure 1. - Conceptual schematic sketches of supersonic commercial aircraft utilizing jet-shock noise shielding by the wing.

E-8771

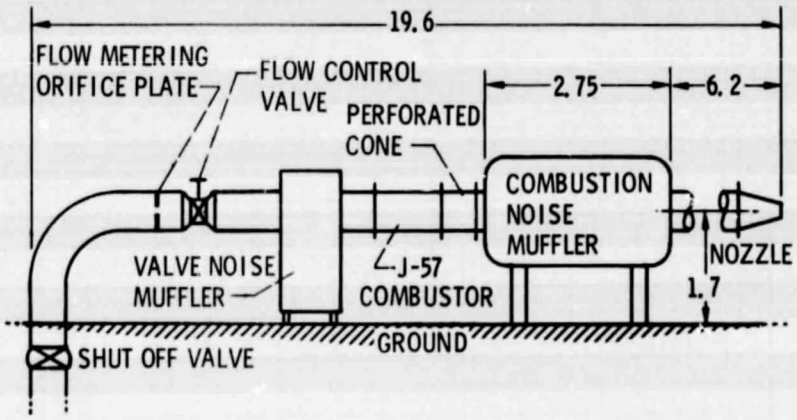

Figure 2. - Schematic sketch of test facility (not to scale). All dimensions in meters.

PRECEDING PAGE BLANK NOT FILMED

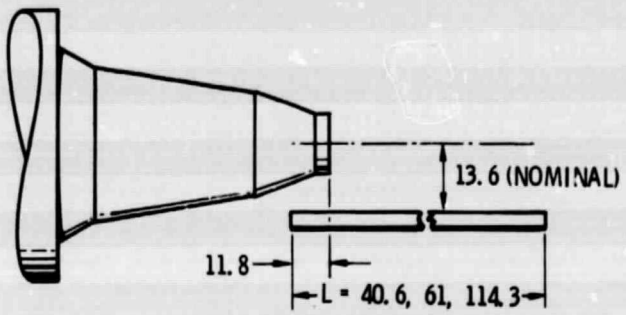

(a) NOZZLE OVER WING.

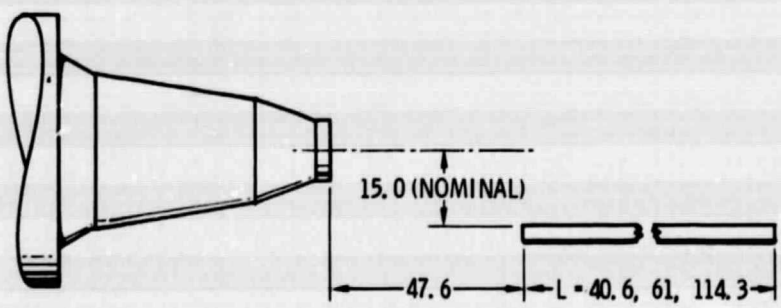

(b) NOZZLE AHEAD OF WING.

Figure 3. - Schematic sketches of nozzle/wing configurations (not to scale). Dimensions in centimeters.

E-8771

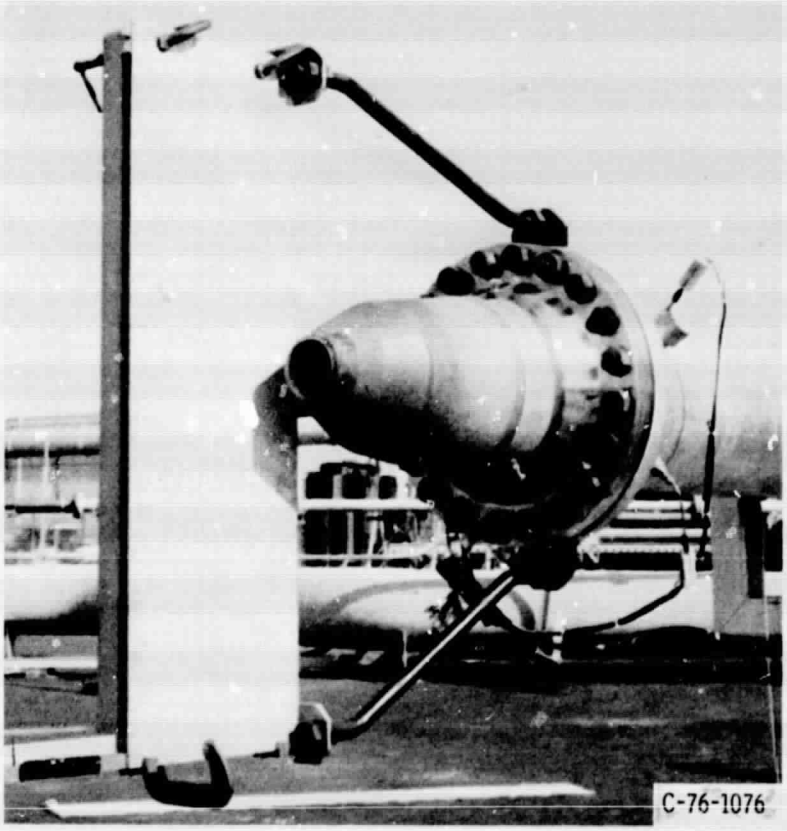

Figure 4. - Nozzle/wing configuration (nozzle over wing placement) installed ontest site.

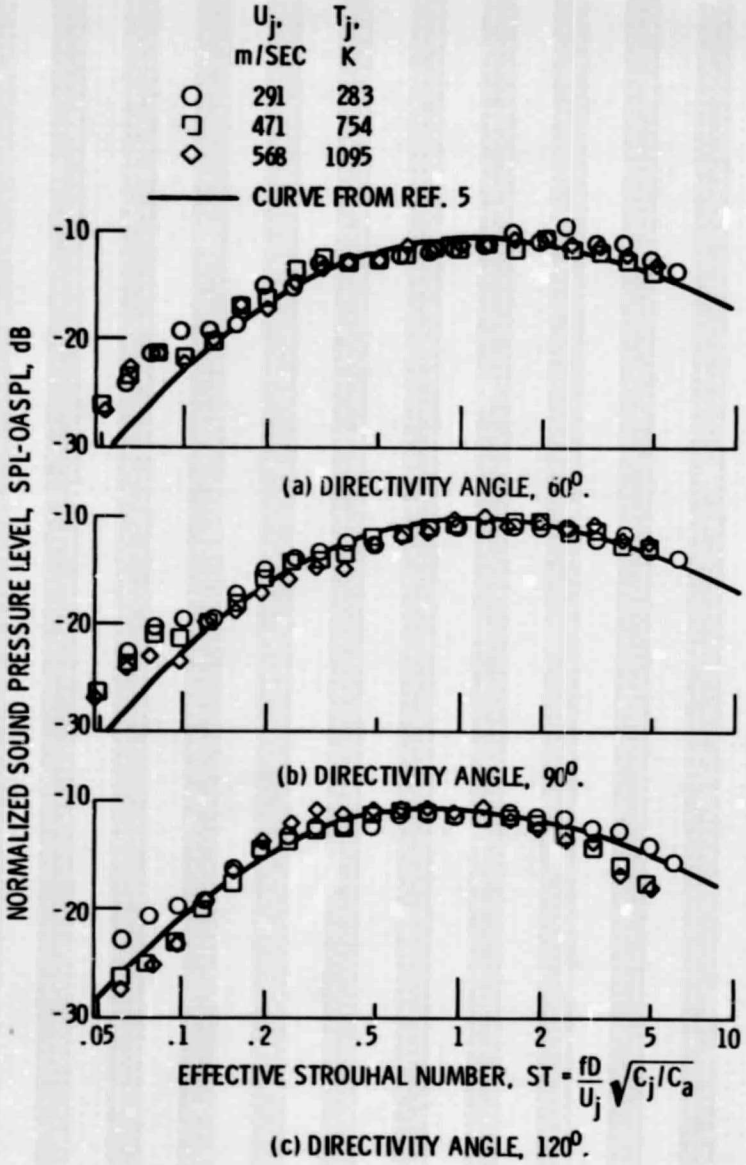

Figure 5. - Sound pressure level spectra for subsonic jet flow. M_j, 0.94; nozzle alone.

NORMALIZED OVERALL SOUND PRESSURE LEVEL, OASPL - 10 LOG $\left[\left(\frac{A_j}{R^2}\right)\left(\frac{\rho_a}{\rho_{ISA}}\right)\left(\frac{C_a}{C_{ISA}}\right)^4\right]$ - 10 LOG $\left[\frac{3(U_j/C_a)^{3.5}}{0.6 + (U_j/C_a)^{3.5}} - 1\right]$ LOG(ρ_j/ρ_a), dB

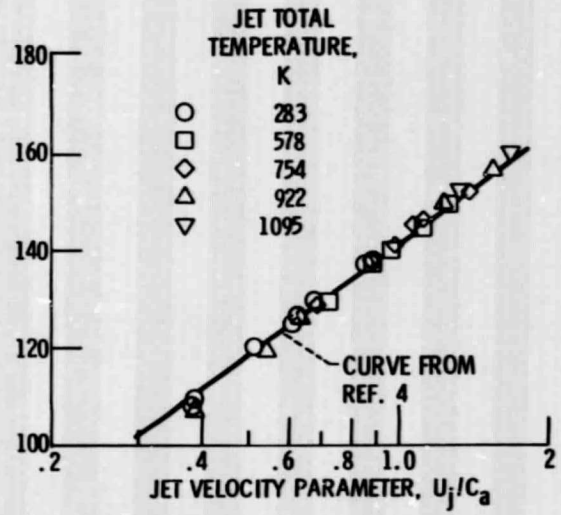

Figure 6. - Comparison of measured OASPL at $\theta = 90^0$ with predicted values from ref. 4; nozzle alone.

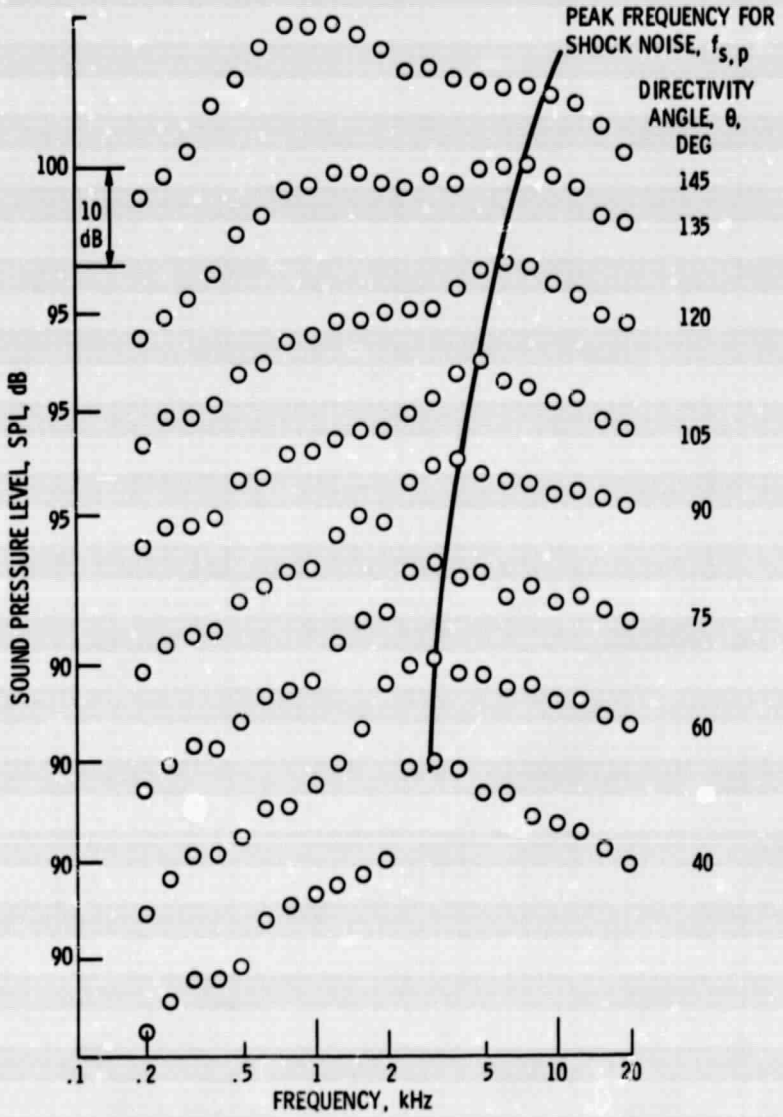

Figure 7. - Typical variation of shock peak frequency with directivity angle. M_j, 1.3; T_j, 283 K; nozzle alone.

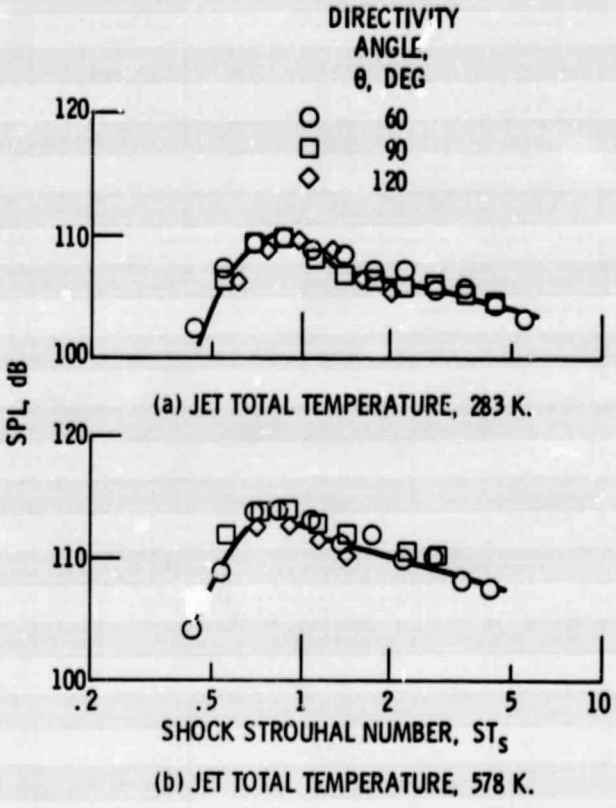

Figure 8. - Representative shock spectra for several directivity angles as a function of shock Strouhal number. Nominal M_j, 1.3; nozzle only.

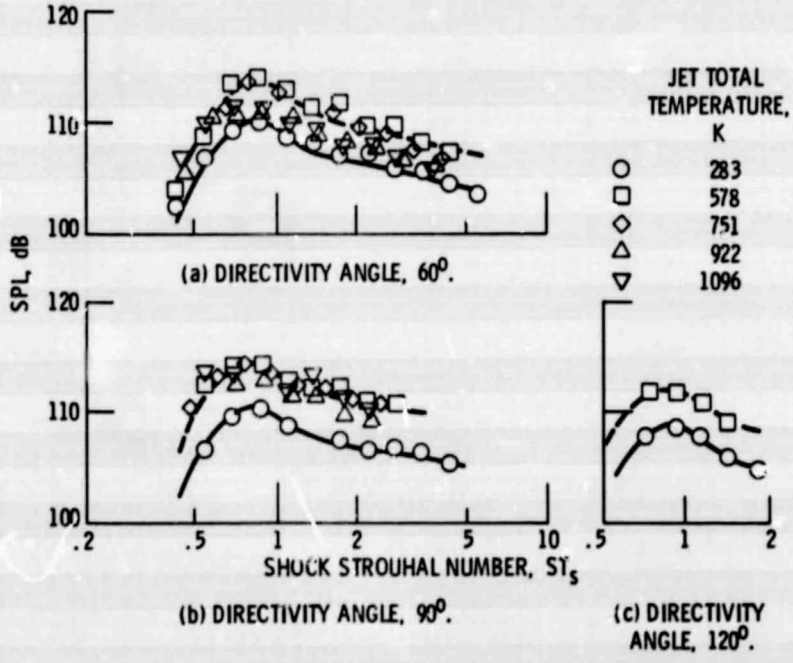

Figure 9. - Effect of jet temperature on shock noise level and spectra. Nominal M_j, 1.3; nozzle alone.

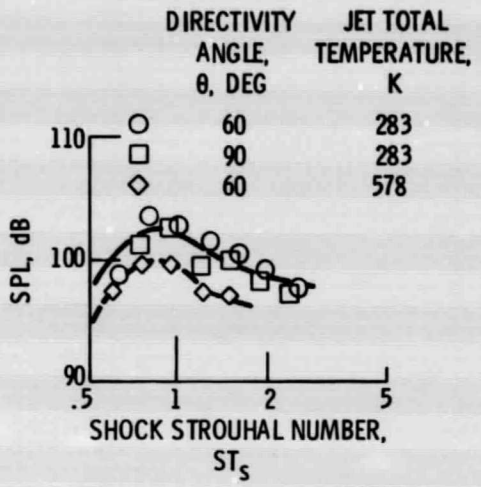

Figure 10. - Representative shock noise spectra as a function of shock Strouhal number. Nominal M_j, 1.09; nozzle alone.

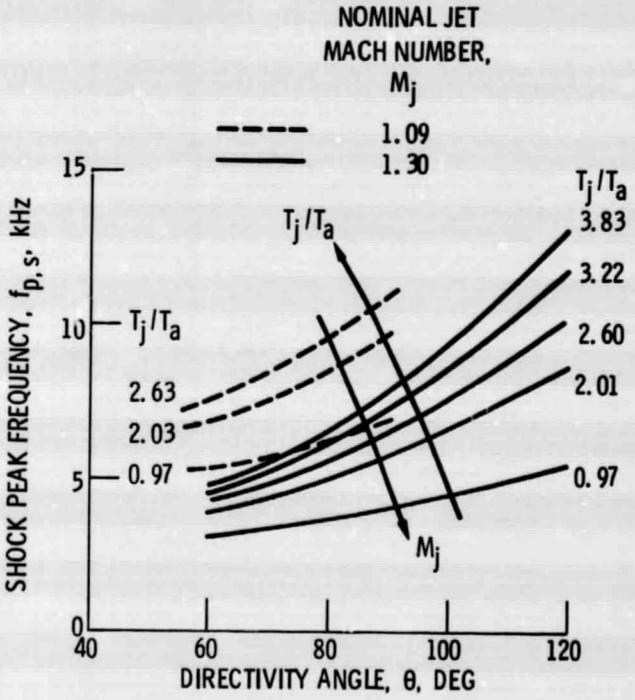

Figure 11. - Variation of shock peak frequency with jet total temperature and jet Mach number; Nozzle alone.

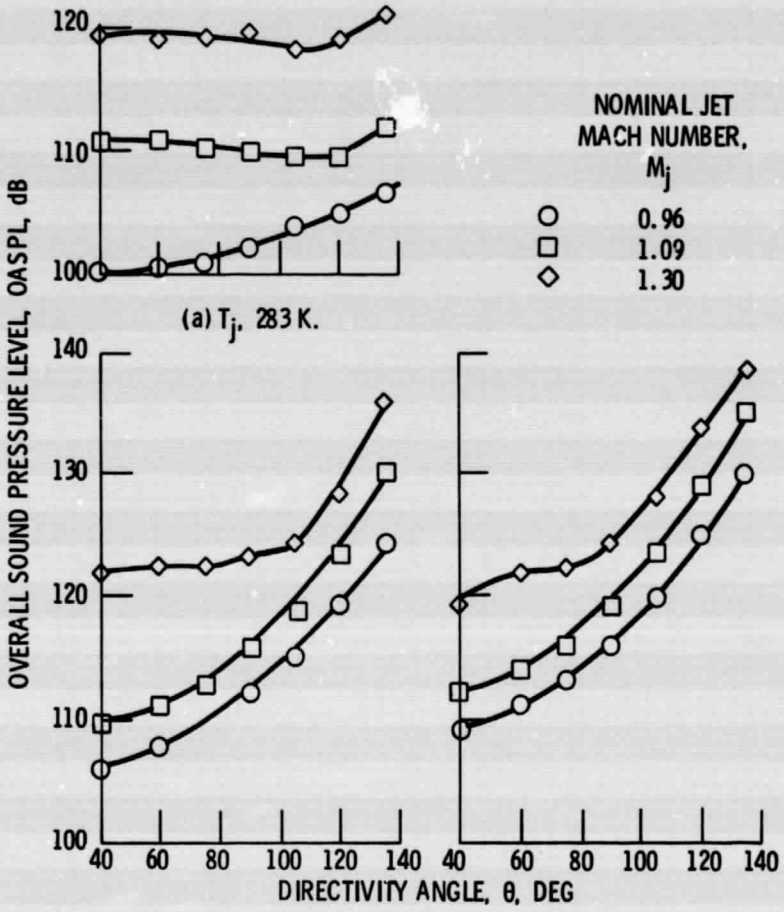

Figure 12. - Representative variations of OASPL with jet total temperature, T_j, jet Mach number, M_j, and directivity angle, θ, nozzle alone.

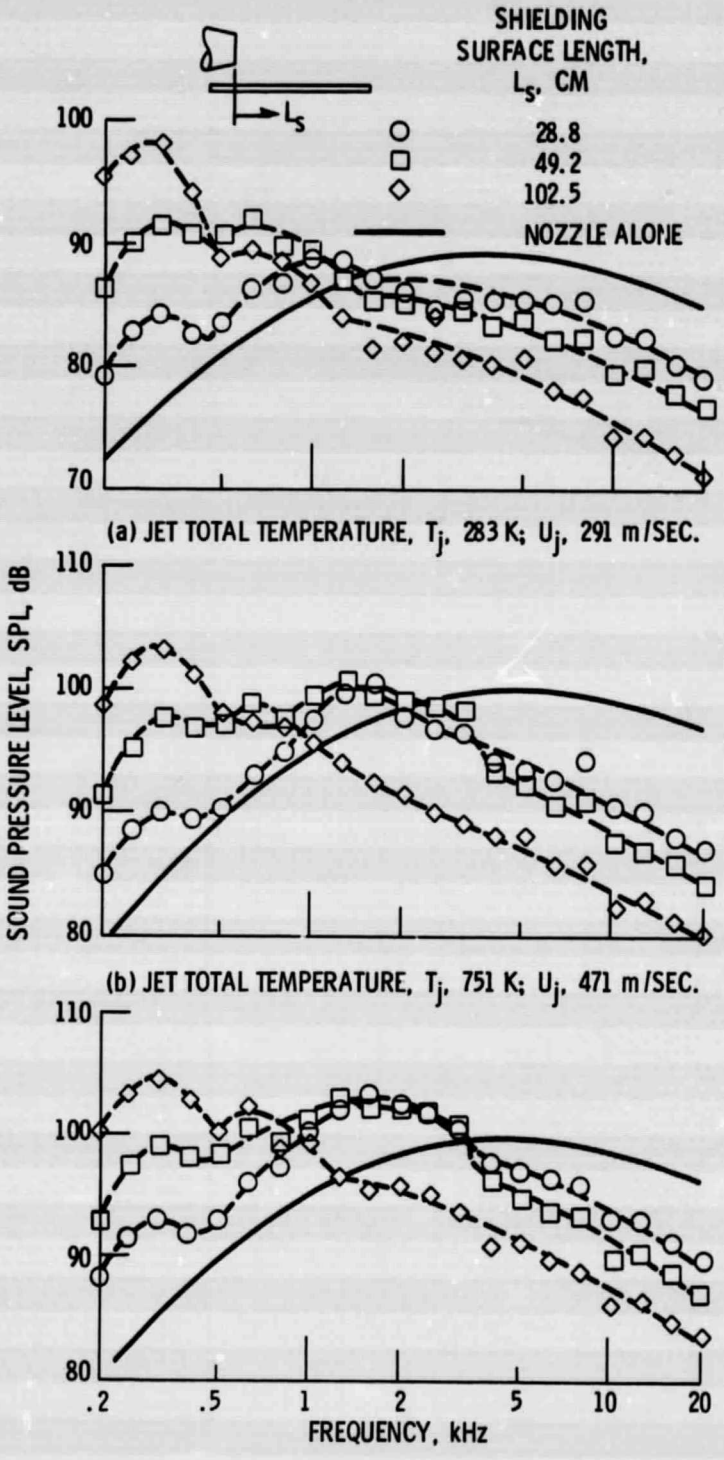

(a) JET TOTAL TEMPERATURE, T_j, 283 K; U_j, 291 m/SEC.

(b) JET TOTAL TEMPERATURE, T_j, 751 K; U_j, 471 m/SEC.

(c) JET TOTAL TEMPERATURE, T_j, 1096 K; U_j, 568 m/SEC.

Figure 13. - Effect of shielding surface length and jet total temperature on spectra with subsonic jet velocities. M_j, 0.94; θ, 60^0.

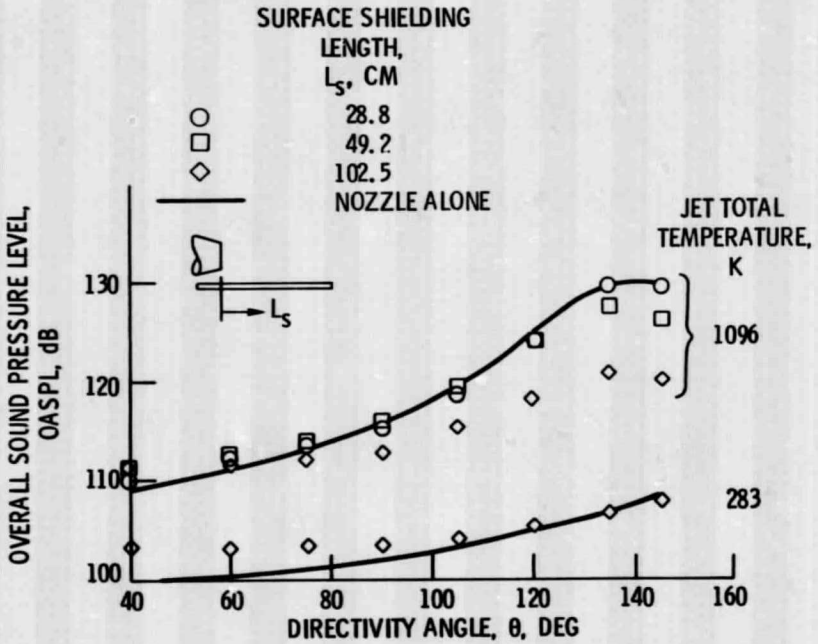

Figure 14. - Representative variation of OASPL for nozzle/wing configurations as a function of directivity angle; M_j, 0.94.

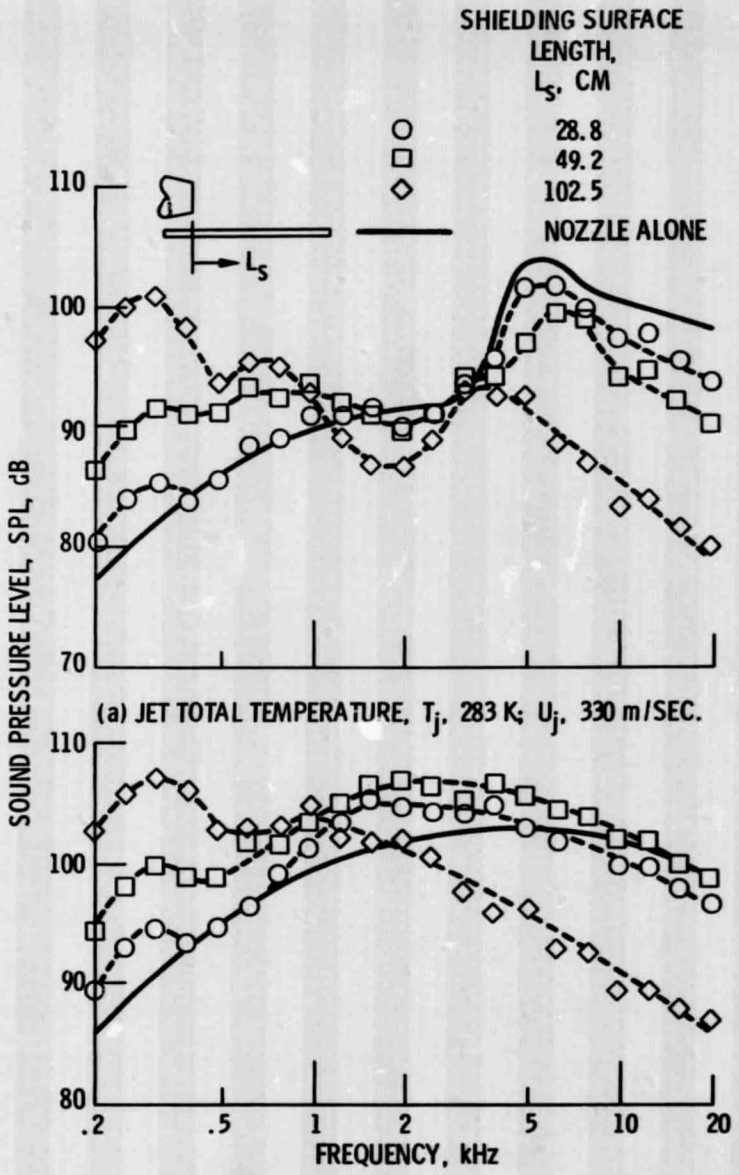

Figure 15. - Effect of shielding surface length and jet total temperature on nozzle/wing spectra with low supersonic jet velocities; M_j, 1.09; θ, 60^0.

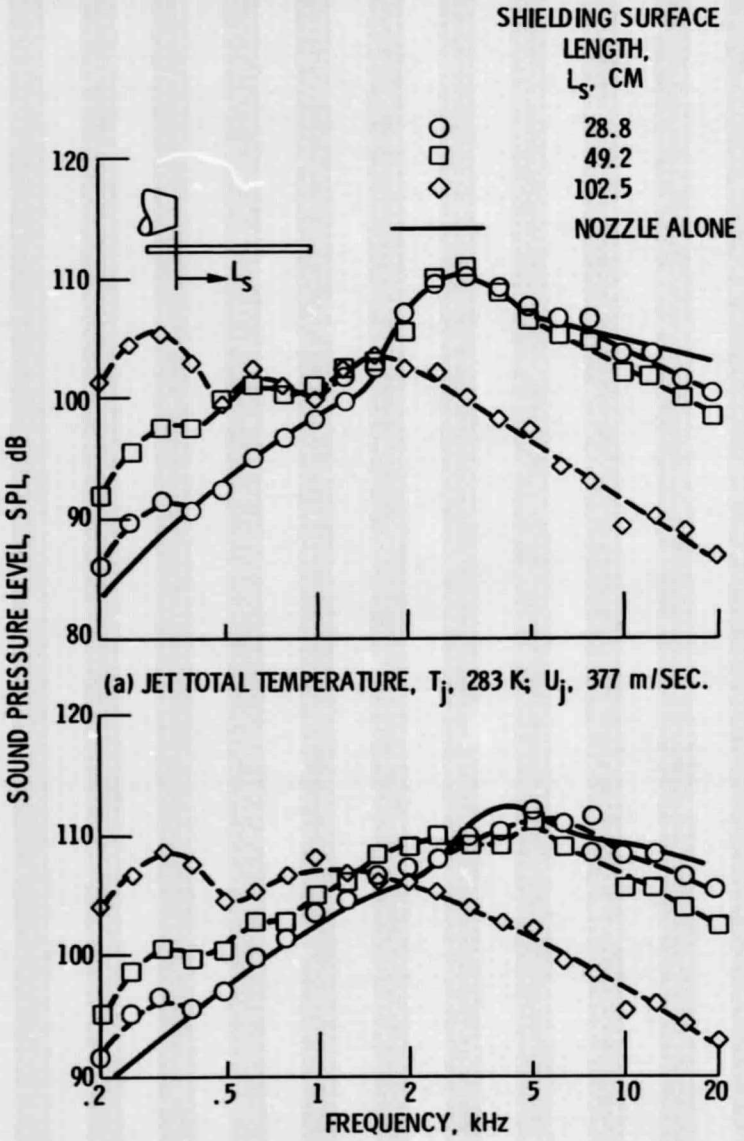

Figure 16. - Effect of shielding surface length and jet total temperature on nozzle/wing spectra for a supersonic jet Mach number, M_j, of 1.3; θ, 60^0.

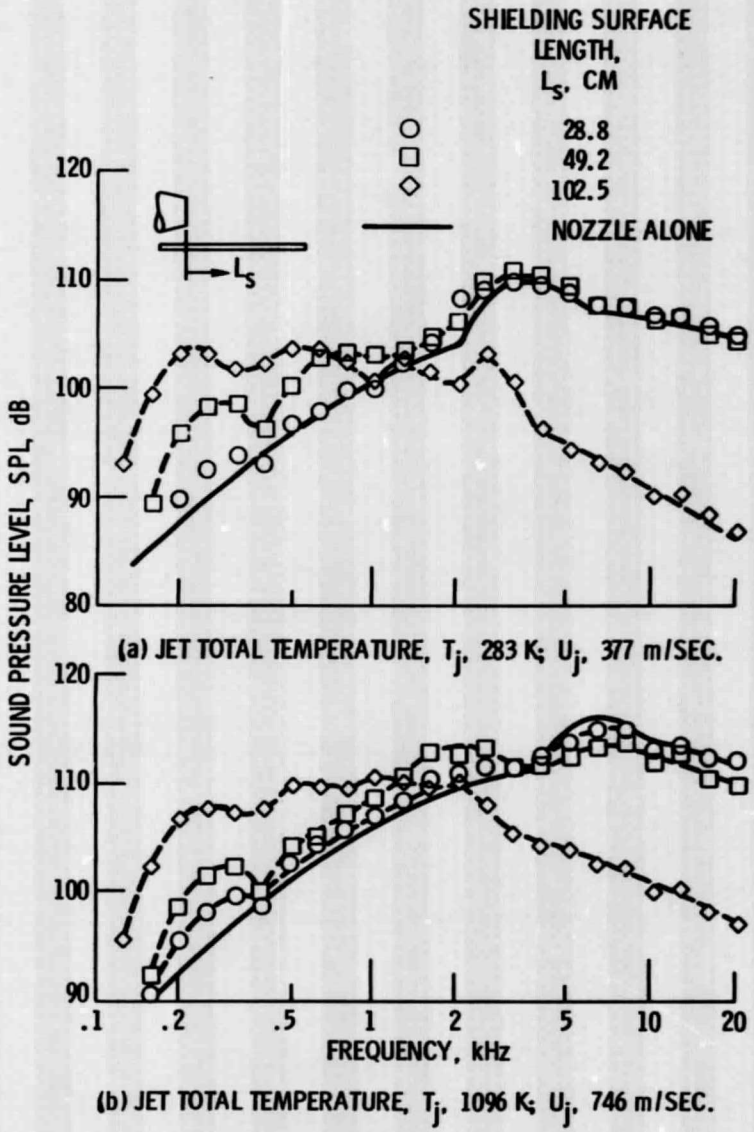

Figure 17. - Effect of shielding surface length and jet total temperature on nozzle/wing spectra for a supersonic jet Mach number of 1.3; θ, 90^0.

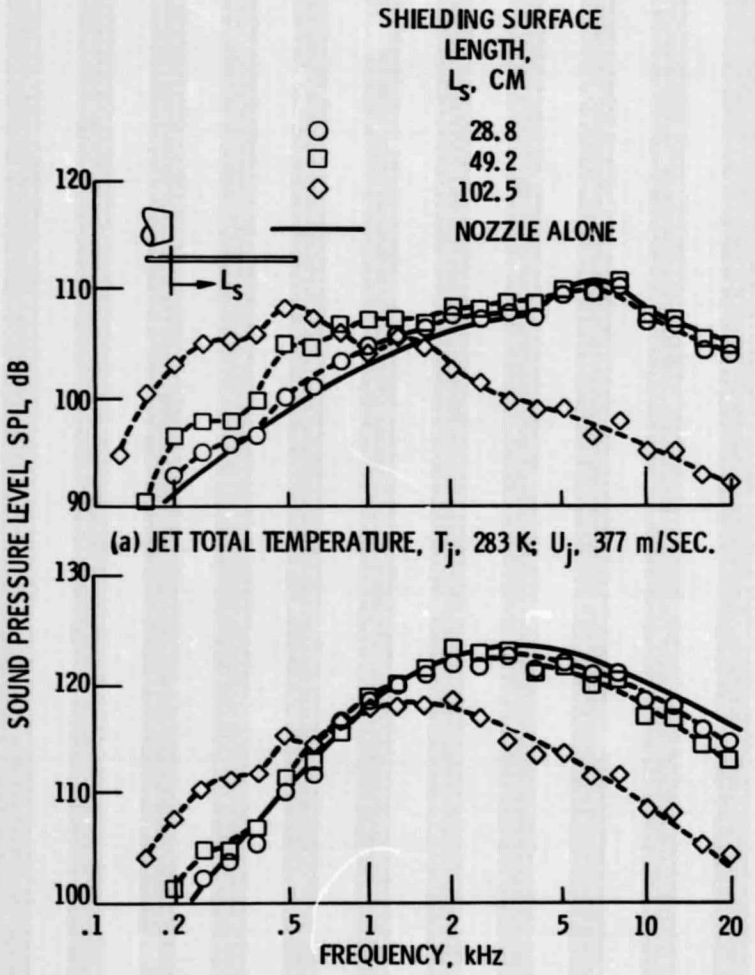

(a) JET TOTAL TEMPERATURE, T_j, 283 K; U_j, 377 m/SEC.

(b) JET TOTAL TEMPERATURE, T_j, 1096 K; U_j, 746 m/SEC.

Figure 18. - Effect of shielding surface length and jet total temperature on nozzle/wing spectra for a supersonic jet Mach number of 1.3; θ, 120°.

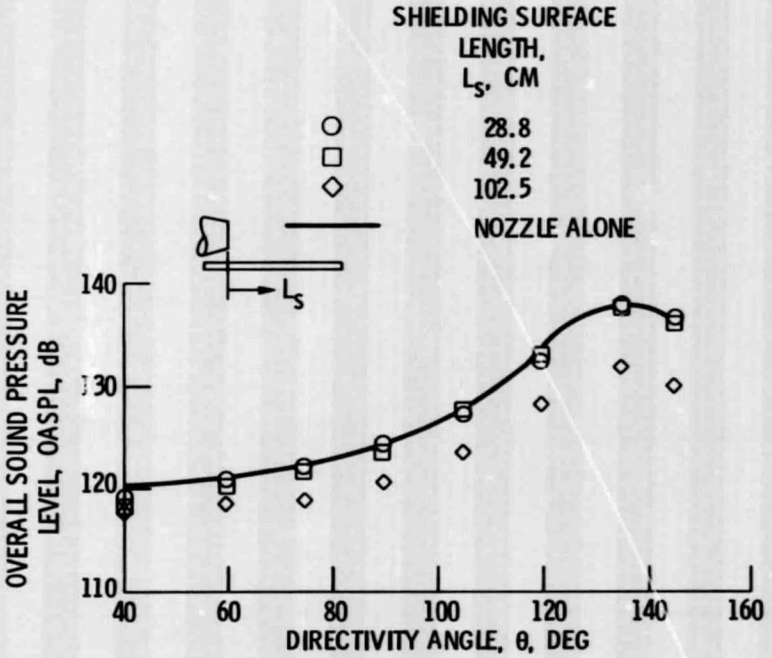

Figure 19. - Representative variation of OASPL for nozzle/wing configurations as a function of directivity angle. M_j, 1.3; T_j, 1096 K; nozzle over wing.

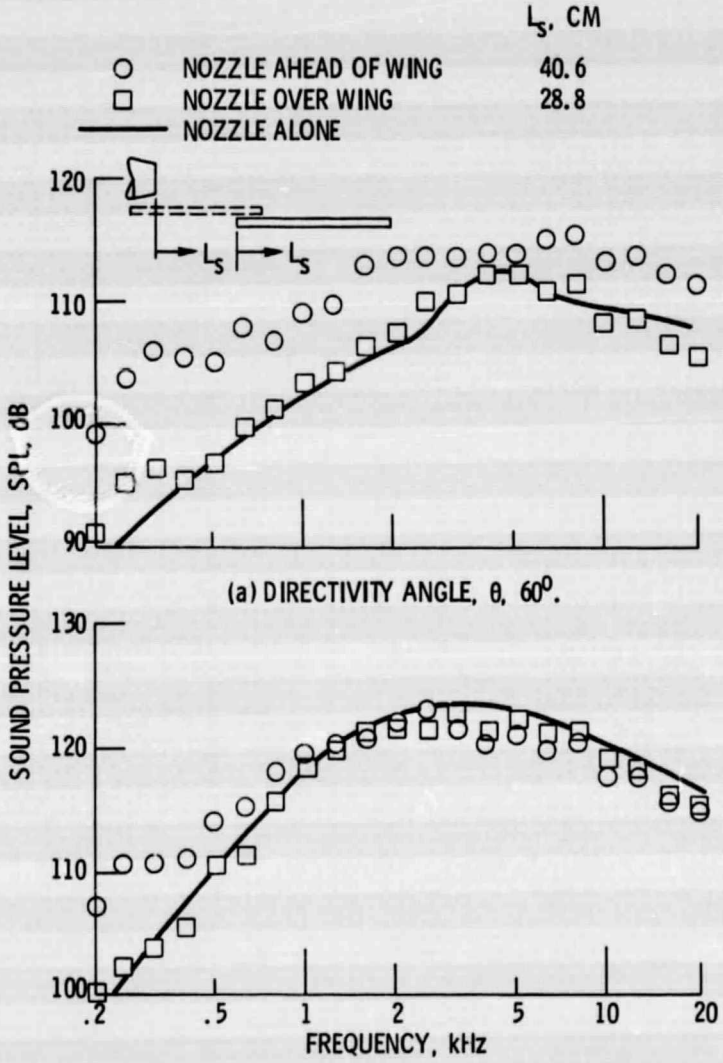

Figure 20. - Comparisons of nozzle/wing spectra for nozzle placements ahead of and over the wing with short wings; M_j, 1.3; T_j, 1096 K.

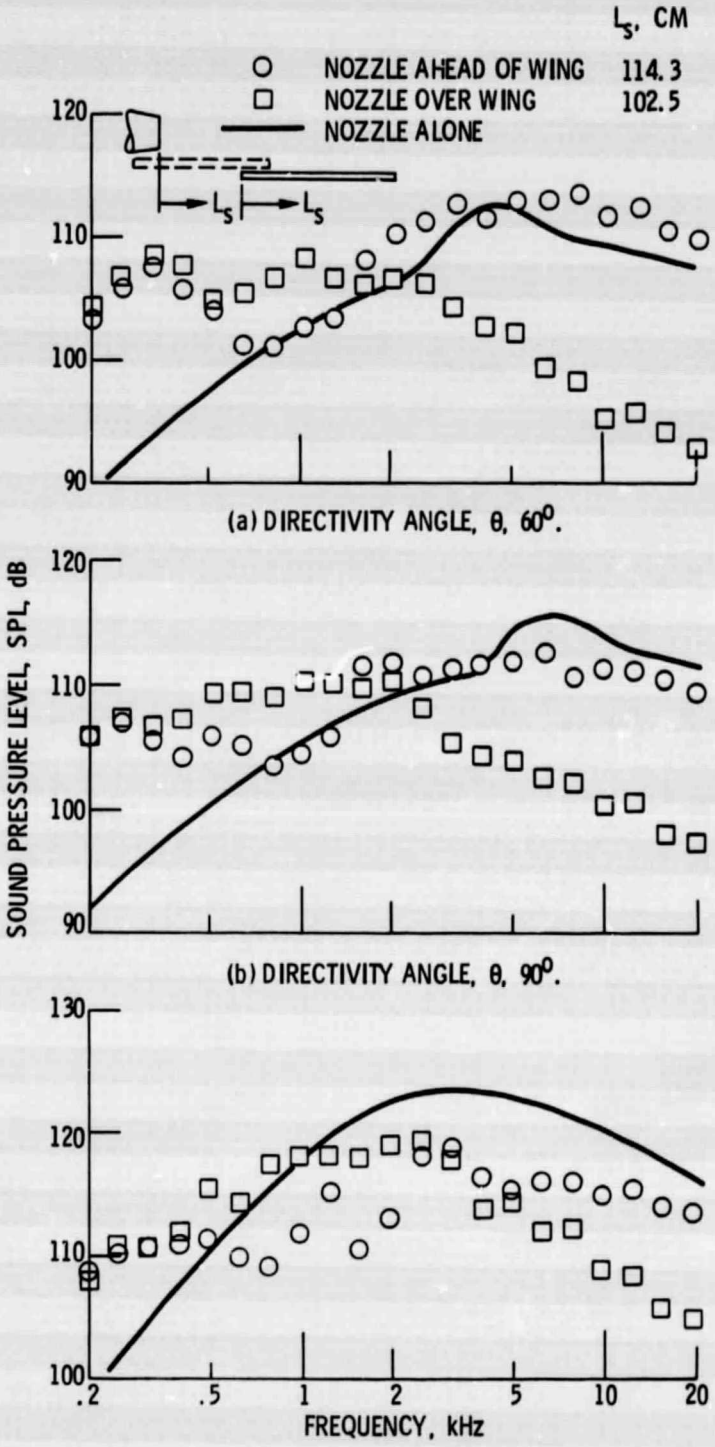

Figure 21. - Comparisons of nozzle/wing spectra for nozzle placements ahead of and over the wing with long wings. M_j, 1.3; T_j, 1096 K.

E-8771

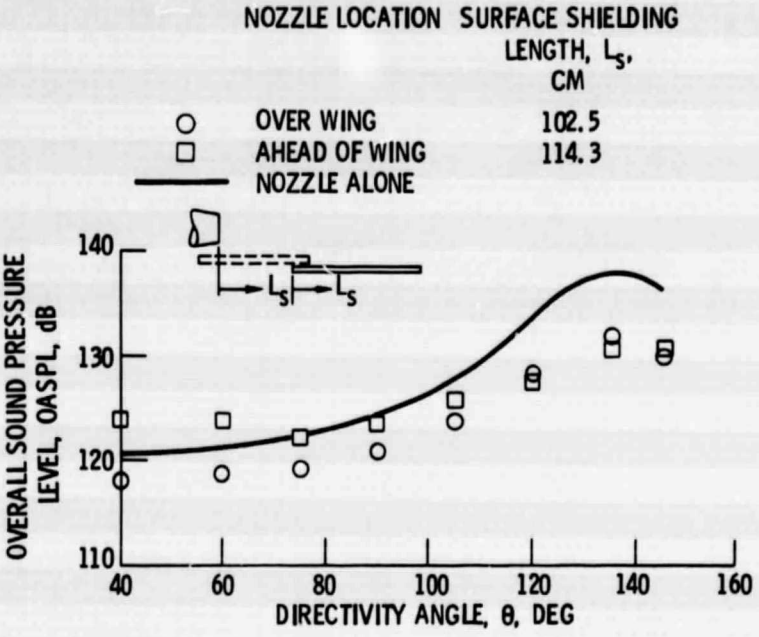

Figure 22. - Comparison of OASPL for nozzle ahead of wing with OASPL for nozzle over wing and nozzle only as a function of directivity angle. M_j, 1.3; T_j, 1096 K.